Biosensors and Bioelectronics 38 (2012) 252–257

Contents lists available at SciVerse ScienceDirect

Biosensors and Bioelectronics

journal homepage: www.elsevier.com/locate/bios

# Nanoporous gold electrode as a platform for the construction of an electrochemical DNA hybridization biosensor

Laleh Enayati Ahangar, Masoud A. Mehrgardi *

*Department of Chemistry, Faculty of Science, University of Isfahan, Isfahan 81746-73441, Iran*

ARTICLE INFO

*Article history:*
Received 18 March 2012
Received in revised form
28 May 2012
Accepted 29 May 2012
Available online 7 June 2012

*Keywords:*
DNA hybridization biosensor
Nanoporous gold electrode
Ferrocene-modified DNA
Thermodynamically stable mismatches
Charge transfer in DNA

ABSTRACT

The application of a nanoporous gold electrode (NPGE) in the fabrication of an electrochemical sensing system for the detection of single base mismatches (SBMs) using ferrocene-modified DNA probe has been investigated in the present manuscript. Ferrocene carboxylic acid is covalently attached to the amino-modified probe using EDC/NHS chemistry. By covalent attachment of the redox reporter molecules on the top of DNA, the direct oxidation of the ferrocene on the electrode surface is avoided. On the other hand, the electrochemical signals are amplified by anodizing the electrode surface and converting it to nanoporous form. By improving the sensitivity of the biosensor, the different SBMs including the thermodynamically stable G–A and G–T mismatches, can be easily distinguished. In this research, NPGE was prepared by anodization and chemical reduction of Au surface and used for signal amplification. Nanoporous electrode enhances the sensitivity of DNA biosensor and makes it capable to detect complementary target DNA in sub-nanomole scales.



## 1. Introduction

In genetic researches, detection of variations in the gene sequences such as single nucleotide polymorphisms is very critical (Zhang et al., 2010) and a variety of methods such as optical (Peterson et al., 2002), acoustic (Hook et al., 2001), voltammetric (Cai et al., 2002; Gaoa et al., 2010; Gong et al., 2009; Ihara et al., 1997; Wang et al., 2008; Zhang et al., 2005) and electrochemical impedance spectroscopic (Gong et al., 2009; Li et al., 2005, 2006, 2007; Long et al., 2004; Wang et al., 2008) approaches have been developed. Many strategies including allele-specific hybridization (Xiao et al., 2007), hairpin conformational changes (Farjami et al., 2011; Gong et al., 2009; Wang et al., 2008), junction-probe (Zhang et al., 2010), charge transport (CT) through DNA (Boon et al., 2002; Gorodetsky et al.,2007, 2008a; Kelley et al.,1997, 1999a, 1999b; Polsky et al., 2006; Wong and Gooding, 2006), have been used for the genotyping. CT through DNA is one of the most important strategies for detection of single base mismatches (SBM) (Wong and Gooding, 2006). Barton's group pioneers in the field of conductive properties of duplex DNA for the sensing application (Kelley et al., 1997, 1999a, 1999b) and then this was followed by several groups (Polsky et al., 2006; Wong and Gooding, 2006). CT through duplex is very sensitive to $\pi$-stacking and is used in mutational assays based on the perturbation in base-stacking such as mismatches (Gorodetsky et al., 2008a). In this strategy, a redox active compound is covalently bound to the top of the DNA or non-covalently bond to the DNA (Gorodetsky et al., 2007). This electroactive label could be efficiently reduced or oxidized but in the presence of a SBM, its electrochemical signal switches off (Boon et al., 2002). Covalently attached reporter is employed more than the other protocols, for their two main advantages. First, they do not diffuse and do not interact before the SBM position; therefore, they do not show a signal in the presence of a SBM. Moreover, this type of reporters could not achieve the electrode surface via the pinholes. Consequently, by this strategy the thermodynamically stable G–A and G–T mismatches could be easily detected (Mehrgardi and Daneshtalab, 2011). Different redox-active molecules such as Redmond red (Boon et al., 2000), daunomycin (Kelley et al., 1999b), nile blue (Gorodetsky et al., 2008c), anthraquinone (Di Giusto et al., 2004), osmium tetraoxide complexes (Fojta et al., 2006) and ferrocene (Fan et al., 2003; Ge and Levicky, 2010) were used as a covalently attached reporter.

Barton et al. used Redmond red (Boon et al., 2000) and Nile blue (Gorodetsky et al., 2008b) to detect abasic sites in DNA. Ferrocene was used widely for its electrochemically reversible behavior, its amenability to derivatization and good stability (Ge and Levicky, 2010). Ferrocene-modified DNA can be synthesized using different strategies: by covalent attachment of a ferrocenyl group to the 5′-aminohexyl terminated DNA, by solid phase coupling of a ferrocene to a DNA containing 5′-iodoudine, and by replacing a nucleotide by a ferrocene unit during solid phase DNA synthesis (Sassolas et al., 2007).

Willner's group utilized ferrocene as a label for DNA replica. They used polymerase induced generation and then the redox-active

* Corresponding author. Tel.: +98 311 7932710; fax: +98 311 6689732.
*E-mail address:* m.mehrgardi@chem.ui.ac.ir (M.A. Mehrgardi).

0956-5663/$ - see front matter © 2012 Elsevier B.V. All rights reserved.
http://dx.doi.org/10.1016/j.bios.2012.05.040

replica is coupled to the glucose-oxidase. This method provides the bioelectrocatalytic amplification of the DNA detection (Patolsky et al., 2002).

Levicky et al. used bioconjugatable ferrocenes for labeling of biomolecules such as DNA (Ge and Levicky, 2010). Furthermore, Heeger and Plaxco used a molecular beacon-like DNA stem-loop labeled with ferrocene for sequence-specific detection of DNA (Fan et al., 2003). Meade's groups applied ferrocene-modified probes for electronic detection of SBM. They employed alternating current voltammetry at the first harmonic (Yu et al., 2001). The same group used a ferrocene-modified oligonucleotide and an electrochemical system based on the formation of complementary sandwich type complex for detection of SBM (Ihara et al., 1997).

Thermodynamically stable mismatches such as G–A and G–T mismatches could not have an effect on the charge transfer dramatically; therefore for their detection, an improvement in biosensor sensitivity was needed. There are several methods for amplification of signals such as electrocatalytic amplification, bioelectrocatalysis using enzymatic assays and using metal nanoparticles (Mehrgardi and Ahangar, 2011) and nanoporous structure (Chang et al., 2011; Hu et al., 2008; Jia et al., 2007); recently nanoporous electrodes have been found interesting (Rho et al., 2008; Vlassiouk et al., 2005; Zhong et al., 2011), especially nanoporous gold electrode (Hu et al., 2008) due to its properties.

In this study, nanoporous gold electrode (NPGE), to fabricate an electrochemical sensing system for the detection of single base mismatches using ferrocene-modified DNA probe, has been investigated and described. Ferrocene carboxylic acid was covalently attached on top of amino labeled probe by forming carbodimide bond using EDC/NHS chemistry. The nanoporous gold electrode amplified the signal of biosensor; therefore, the capability of this DNA biosensor was examined for lower concentration of DNA target and detection of mismatches containing G–A, G–T, C–A and T–T mismatch targets.

## 2. Experimental

### 2.1. Materials

Ferrocene carboxylic acid (FCA), N-hydroxylsuccinimide (NHS), N-(3-dimethylaminopropyl)-*n*-ethyl carbodimide hydrochloride (EDC), 6-mercaptohexanol (MCH), tris(2-carboxyethyl) phosphine HCl (TCEP), nitric acid, sulfuric acid, sodium dihydrogen phosphate, disodium hydrogen phosphate, sodium chloride, magnesium chloride and ascorbic acid were purchased from commercial sources (Merck or Sigma) and used as received, without further purification. The distilled-deionized water was used in all solution preparations (18 MΩ).

The stock solution of the oligonucleotides (4 μM) was prepared with PBS buffer solution and kept frozen at −20 °C. All experiments were performed at room temperature in a three-electrode electrochemical cell. In this study, DNA oligonucleotides were obtained from Eurofins MWG/Operon Co. and had the following sequence:

Capture: 5′–HS-TCACTGCAAA–3′
Probe: 5′–CTCATGGTCC-$NH_2$–3′
Complementary: 5′–GGACCATGAGTTTGCAGTGA–3′
NON-complementary: 5′–ATCTACTACTGCATTCCGTC–3′
G–A mismatch: 5′–GGAC**A**ATGAGTTTGCAGTGA–3′
G–T mismatch: 5′–GGACC**G**TGAGTTTGCAGTGA–3′
C–A mismatch: 5′–GGACCA**C**GAGTTTGCAGTGA–3′

Electrochemical experiments were carried out using an Autolab electrochemical system PGSTAT 30 [ECO CHEMIE, The Netherlands] driven by the GPES software. A conventional three-electrode system, consisting of small parts of gold recordable compact disks (CD-R) as working electrode (Angnes et al., 2000; Kiani and Fard, 2009), a platinum wire as an auxiliary electrode and an Ag/AgCl/3.0 M KCl reference electrode was used for experiments.

### 2.2. Preparation of the nanoporous gold electrode (NPGE)

The gold electrode was prepared from small pieces of recordable compact disk (CD) made of gold (Angnes et al., 2000; Kiani and Fard, 2009). Briefly, a small cut of CD was placed in nitric acid for removing the protective layer of the CD and it was washed with water thoroughly. Then it secured to the bottom of a Teflon cell with an o-ring. The exposed gold surface was used as a working electrode. The gold electrode was electrochemically cleaned with 0.01 M NaOH.

The NPGE was prepared according to previous methods (Jia et al., 2008; Kiani and Fard, 2009), briefly; the NPGE was constructed in two steps. In the first step, the gold surface of reflective layer of CD was anodized in a phosphate buffer solution (pH 7.4) for 3 min, by applying a step potential of 3.6 V vs. Ag/AgCl. During the anodizing procedure, gas bubbles are produced on the CDtrode surface, these bubbles were removed by striking the cell during the anodizing. In the second step, the anodized gold surface was reduced using a fresh solution of 1.0 M of ascorbic acid for 5 min. The color of the CDtrode surface

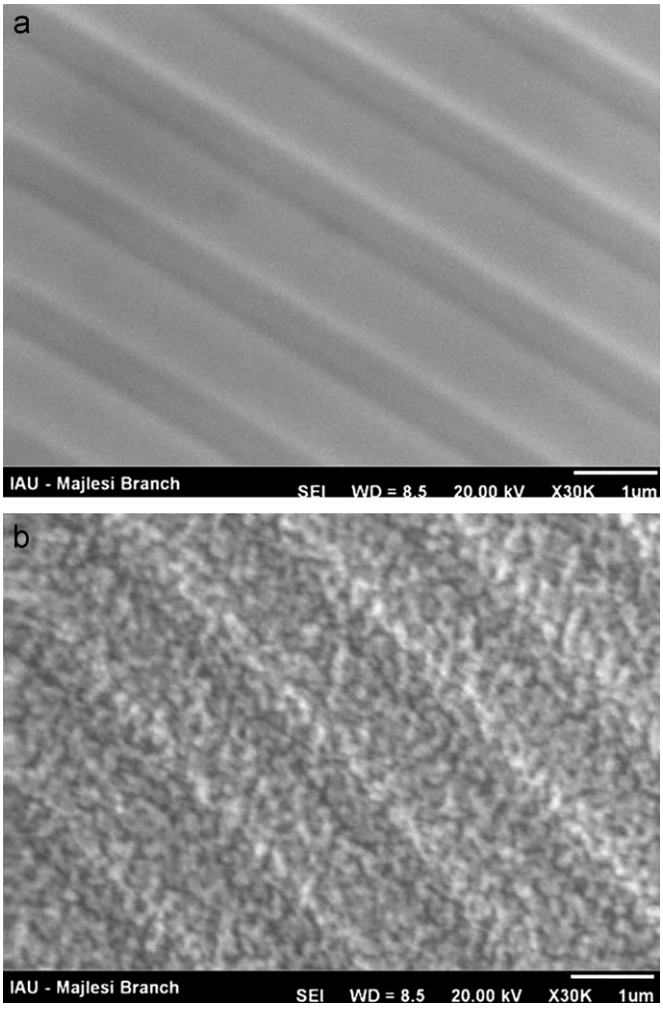


**Fig. 1.** SEM images of (a) bulk gold CDtrode and (b) NPGE.

changed to dark due to construction of nanoporous structure. Ascorbic acid reduces the gold oxide to metallic gold.

The surface area of the gold CDtrode before and after porosity was measured by following their cyclic voltammograms in 0.5 M of sulfuric acid, by assuming a specific charge of 386 μC/cm for the reduction peak of gold electrode surfaces. The surface areas before and after porosity were $0.19 \pm 0.01$ and $0.69 \pm 0.02$ $cm^2$ respectively.

Fig. 1 shows the SEM images of bulk gold CDtrode and NPGE. The parallel grooves on the electrode are the grooves of CD and the pore size of porous gold electrode is between 60 and 130 nm.

### 2.3. Fabrication of ferrocene-modified DNA biosensor

The prepared NPGE was electrochemically treated in 0.01 M of NaOH and 0.5 M of $H_2SO_4$. The thiol modified capture DNA was deprotected using a previously reported procedure (Gong et al., 2009). Briefly, 75 μL capture DNA (2.5 μM) and 25 μL TCEP solution (0.4 mM) in PBS with pH 7.4 were mixed in a dark place and kept for 1 h to convert S–S bond to SH group. Then 10 μL of deprotected capture DNA, 5 μL of 2 M $MgCl_2$, and 2 μL of 0.5 M $NaH_2PO_4$ solutions were dropped on the NPGE surface. After 1 h, 2 μL aqueous solution of 4 μM MCH solution was added to the drop on the CDtrode surface. After washing the CDtrode surface, a drop containing 10 μL of 4 μM target DNA and 5 μL of 2 M magnesium chloride was placed on the CDtrode surface for 70 min. The CDtrode was then washed and 4 μM amine-labeled probe DNA (10 μL) and 5 μL magnesium chloride (2 M) were dropped on NPGE for 70 min. The probe is complementary to non-hybridized section of the target and would be hybridized with this part. In the last step, a solution containing 1 mM of FCA (60 μL), 10 mM EDC solution and 16 mM of NHS was put on the CDtrode surface for 7 h in a dark place. The resulting CDtrode was ready for the electrochemical detection. Fabrication procedure of DNA biosensor is illustrated in Scheme 1.

## 3. Results and discussion

The construction of the DNA biosensor based on DNA-mediated CT is a good strategy that enables the scientists to detect DNA lesions in real time methods without using the PCR technique. Covalent attachment of ferrocene at the top of DNA has some advantages such as scrubbing out direct electron transfer between redox active reporter and electrode surface. On the other hand, by amplifying the detection signal by using nanoporous gold electrode as the platform, different types of mismatches can be easily detected. Herein, this hypothesis was examined by hybridization of the immobilized probe with several DNA targets, including different mismatches such as C–A, G–T and G–A.

### 3.1. CV and EIS behavior of CDtrode surface in modification steps

The various steps of electrode surface modification were followed by CV and EIS experiments. The cyclic voltammograms of potassium ferricyanide for the different modification steps have been shown in Fig. 2A. By anodizing of the CDtrode surface and converting to nanoporous form, the surface area and so the oxidation and reduction currents are increased (voltammograms a and b, Fig. 2A). Modification of the CDtrode surface with an immobilized capture DNA increases the peak separation ($\Delta E_p$) of ferricyanide ion and decreases the faradic peak currents ($I_p$). These behaviors are due to the development of negative charges on the CDtrode surface by immobilization of DNA which repel $[Fe(CN)_6]^{3-/4-}$ from the electrode surface. (Fig. 2A, voltammogram c). After hybridization of the immobilized capture DNA with the target and probe, the formation of the ds-DNAs increase the negative charges more and so, the access of ferricyanide ions to the CDtrode surface becomes difficult, the peak separation ($\Delta E_p$) enhances more, and the faradic peak currents ($I_p$) diminish again (Fig. 2A, voltammograms d and e).

EIS is a valuable method for the investigation of electrode surface changes. Immobilization of biomaterial decreases the double-layer capacitance and slows down the interfacial electron-transfer kinetics. Fig. 2B shows the impedance aspects of the CDtrode surface for the various steps of the modifications. Upon the covalent immobilization of the DNA capture the electron transfer resistance ($R_{ct}$) increases (Fig. 2B, plot c). Similar to voltammogram observations, these increases are results of electrostatic repulsion of $[Fe(CN)_6]^{3-/4}$ Probe due to the negatively charged phosphate skeletons of DNA. The electrostatic repulsion

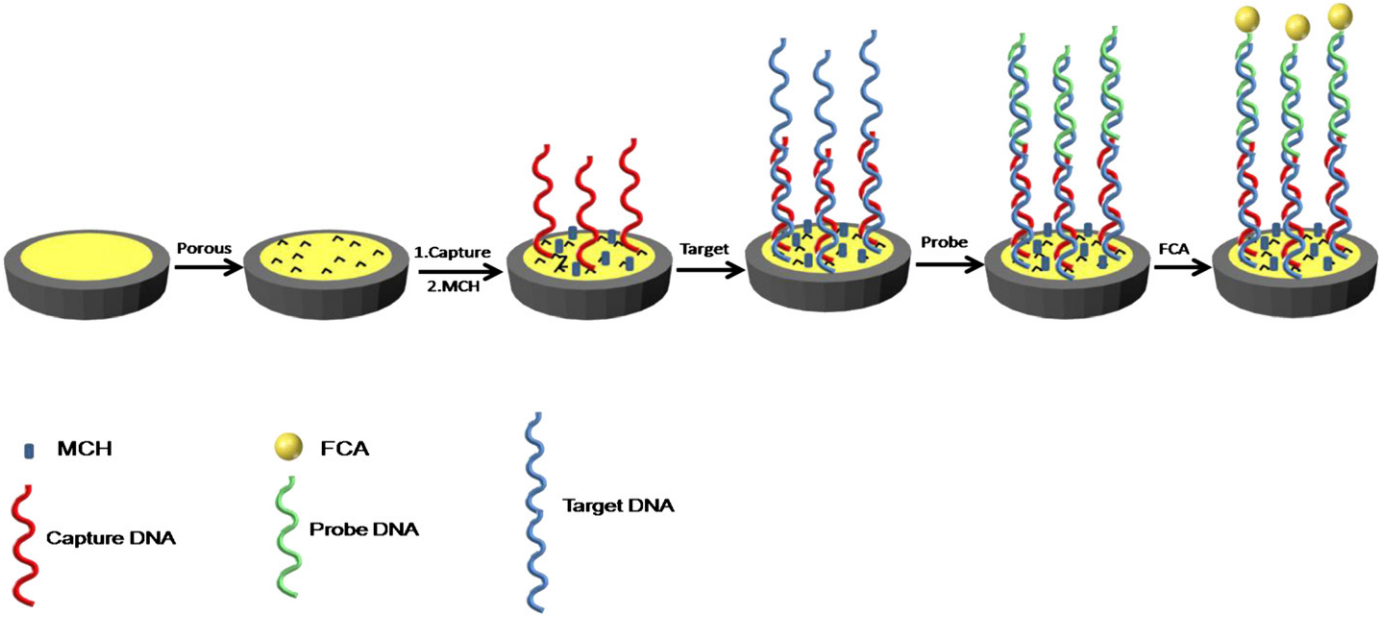


**Scheme 1.** Schematic presentation of the fabrication procedure for the present DNA biosensor.

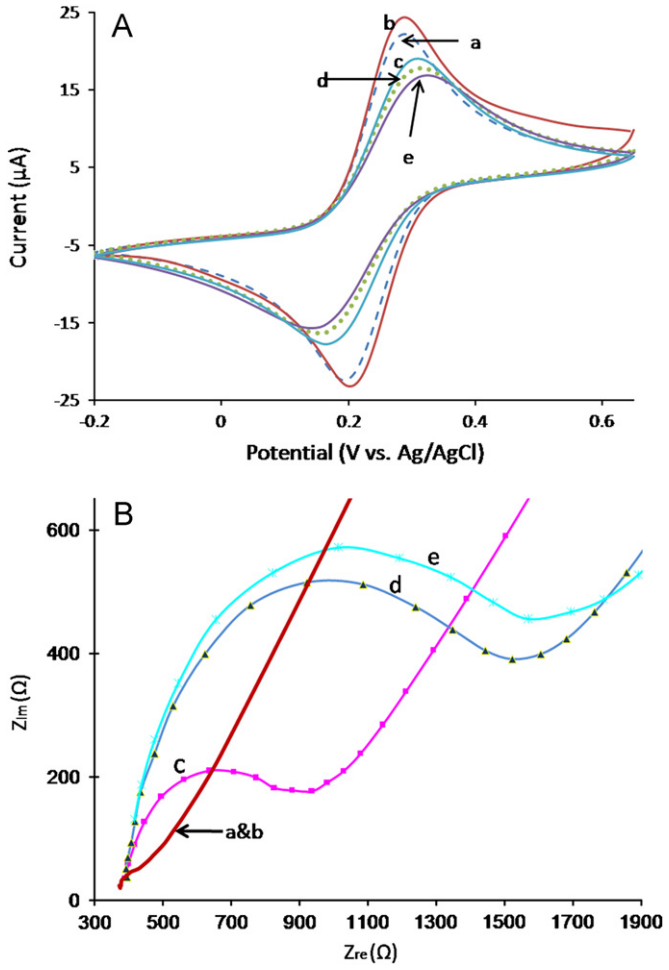


**Fig. 2.** (A) Cyclic voltammograms in the presence of $[Fe(CN)_6]^{3-/4-}$ ($5\times10^{-4}$ M) containing 0.1 M KCl at a scan rate of 100 mV $s^{-1}$ and (B) the Nyquist plots obtained in the presence of $[Fe(CN)_6]^{3-/4-}$ ($5\times10^{-4}$ M; 1:1) as a redox probe at a constant DC potential of O.C.P. for (a) bare gold CDtrode, (b) NPGE, (c) capture immobilization, (d) target hybridization and (e) probe hybridization.

and spatial restriction decrease the kinetics of the electron transfer on the DNA modified complementary target and with the DNA probe (Fig. 2B, plots d and e).

### 3.2. Quantitation of surface density of DNA immobilization

The surface coverage of immobilized DNA at the electrode surface can be obtained by using the number of the adsorbed cationic redox molecules such as ruthenium (III) hexammine (RuHex) on the assembled DNA using a previously reported procedure by Tarlov's group (Steel et al., 1998). Briefly, after the immobilization of DNA on the NPGE surface, the modified electrode was incubated in RuHex solution with low ionic strength (0.02 M KCl). Then for measuring the amount of cationic redox marker, RuHex, a chronocoulometric method was used. Using the Cottrell equation, the chronocoulometric intercept at $t=0$ consists of the double layer charging and the surface excess terms. The surface excess terms are concluded by the variation between the chronocoulometric intercepts for the similar potential step experiment in the presence and absence of redox marker. By following the correlation of the saturated surface excess of RuHex is converted to DNA surface density: $\Gamma_{DNA}=\Gamma_0(z/m)(N_A)$.

Where $\Gamma_{DNA}$ is the probe surface density in molecules/$cm^2$, $m$ is the number of bases in probe DNA, $z$ is the charge of RuHex and $N_A$ is Avogadro's number. Finally, the surface density of probe DNA has been achieved equal to $5\times10^{-12}$ molecules $cm^{-2}$.

### 3.3. Voltammetric transductions

Differential pulse voltammetry (DPV) was used for the investigation of the electrochemical behavior of the covalently attached FCA on the top of DNA monolayer. Its oxidation signal was used for the detection of various target hybridizations. The effect of nanoporous structure on the response of biosensor has been investigated by following the oxidation peak currents of ferrocene on porous and bulk gold electrode when the immobilized probe was hybridized by the complementary target. As shown in Fig. 3A , analytical signal of the assay is significantly enhanced by converting the surface to nanoporous form. Also, the capability of the duplex DNA layer for charge transfer is highly dependent on $\pi$-stacking of ds-DNA. The presence of a SBM will

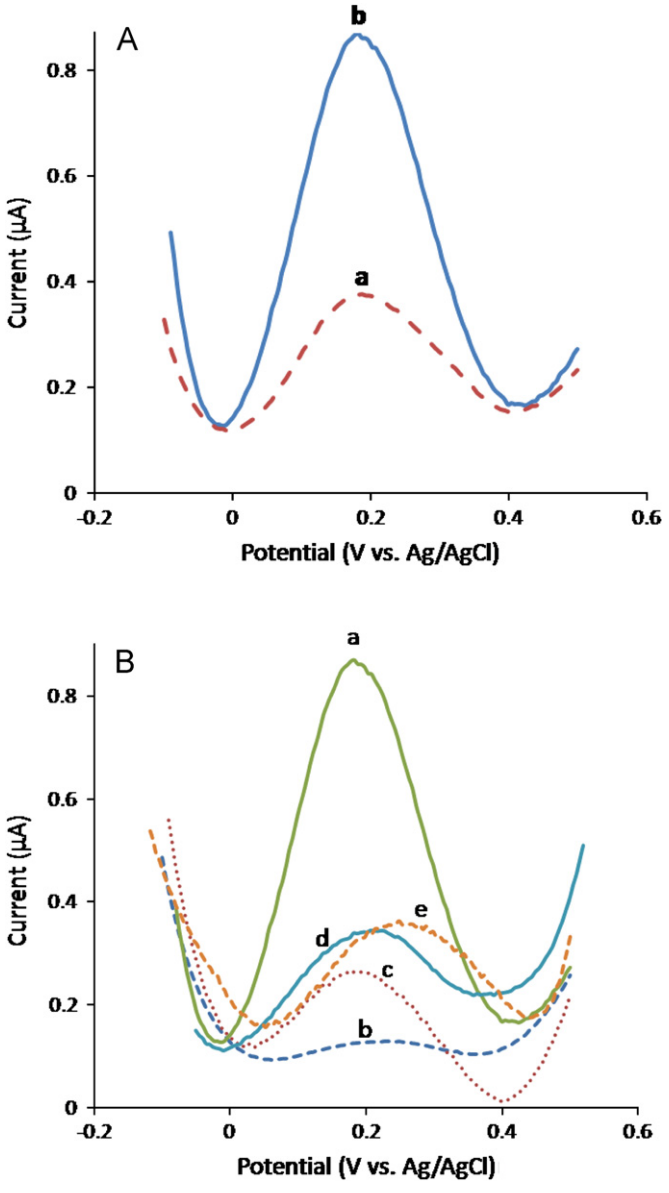


**Fig. 3.** Differential pulse voltammograms of (A) complementary target on (a) bulk gold electrode and (b) NPGE and (B) (a) complementary target (b) non-complementary (c) C–A, (d) G–T and (e) G–A mismatch targets on NPGE at a scan rate of 10 mV $s^{-1}$ and 25 mV amplitude in 0.15 M of KCl and 0.02 M of $NaClO_4$.

disturb the $\pi$-stack and diminish the kinetic of charge transfer remarkably. Fig. 3B shows the voltammograms for the complementary, and non-complementary targets, and targets containing SBM including G–A, G–T and C–A mismatches. Non-complementary target could not hybridize with the immobilized capture and no signal was observed. On the other hand, for the targets containing SBM, a significant decrease in signal of FCA oxidation compared to complementary target is observed. The presence of a single base mismatch disturbs the p-stack of DNA and therefore, the targets containing SBM cannot transfer charge properly; the electrochemical signal of FCA decreased remarkably. As shown in Fig. 3B the peak currents of DPV for G–A, G–T and C–A mismatches are less than 30% of complementary target signal.

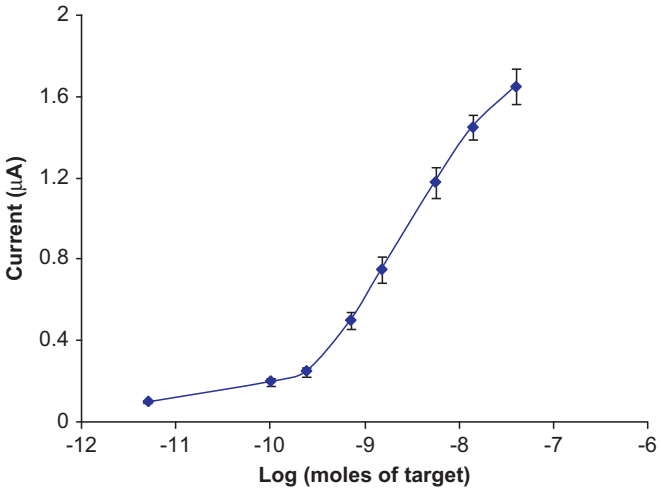


**Fig. 4.** The peak current response of biosensor for the complementary target at different concentrations in DPV analysis, at a scan rate of 10 mV $s^{-1}$ and 50 mV amplitude.

### *3.4. Response characteristics of DNA biosensor for target DNA concentration*

Different concentrations of DNA targets were hybridized with capture DNA on the CDtrode surface and the analytical performance of the biosensor was investigated. A 10 μL aliquot of the target solution over the range from $3.5 \times 10^{-13}$ to $4 \times 10^{-11}$ mol was used for the exploration. Fig. 4 demonstrates that the current intensities of the electrochemical oxidation of FCA enhance as the concentration of complementary target amounts increase. The relationship between peak currents of FCA oxidation and the logarithm of the amount of targets is illustrated in Fig. 4. As shown in the figure, by increasing the complementary target concentrations, the anodic peak currents of the electrochemical oxidation of FCA are increased. For the concentrations less than 25 pmol the signal remains constant roughly. Moreover, the results demonstrate that the assay can detect concentrations of the target as low as $25 \pm 5$ ($n$=3) pmol.

## 4. Conclusion

An innovative DNA hybridization biosensor based on the CT in DNA duplex for detection of various SBMs has been described in this manuscript. The nanoporous gold electrode has been applied as the platform for the fabrication of biosensor. Moreover, the covalently attached FCA on top of the probe DNA was used as a redox reporter and the electrochemical oxidation signal of FCA was followed as the analytical signal. By avoiding direct oxidation of the redox reporter molecules on the electrode surface, and amplification of the electrochemical signals using nanoporous electrode, the different SBMs including the thermodynamically stable G–A and G–T mismatches, can be easily distinguished. In Table 1, a comparison between previously reported assays and the present biosensor is listed. In most of the manuscripts, thermodynamically stable mismatches were not investigated.

**Table 1**
Comparison between the proposed assay and other reported sensors for the mismatch detection.

| Method | Analytical technique | Type of mismatch | SBM Signal change (%) | Ref. |
|---|---|---|---|---|
| Immobilizing a hairpin probe | Differential pulse voltammetry | C–A, C–C | 20 | Fu et al. (2005) |
| Off-on electrochemical hairpin_DNA-based genosensor | Differential pulse voltammetry | C–A | 85 | Farjami et al. (2011) |
| Ferrocene-modified oligonucleotide and sandwich-type ternary complex | Differential pulse voltammetry | C–C | 75 | Ihara et al. (1997) |
| Triple stem DNA probe | AC-voltammetry | C–C | 15 | Xiao et al. (2009) |
| DNA-Mediated Electrochemistry of Disulfides | Square wave voltammetry | C–A | 65 | Wong et al. (2005) |
| Nucleic Acid-Functionalized Pt Nanoparticles | Linear sweep voltammograms | C–A | 40 | Polsky et al. (2006) |
| Nanoporous Gold Electrode | Chronocoulometry | G–G | 90 | Hu et al. (2008) |
| A cadmium phosphate-loaded apoferritin nanoparticle probe | Square-wave voltammogram | C–C | 90 | Liu and Lin (2007) |
| Groove binder molecule (CuPcS4), as redox reporte | Differential pulse voltammetry | G–A, G–T, C–A, T–T (far and near type) | 30 | Mehrgardi and Daneshtalab (2011) |
| Unlabeled hairpin DNA probe | Electrochemical impedance spectroscopy | C–C | 60 | Ferreira et al. (2009) |
| Unlabeled hairpin DNA probe in the presence and absence of $Zn^{2+}$ | Electrochemical impedance spectroscopy | C–C, C–A, C–T, G–A, G–G, G–T, T–T, A–A | 50–93 | Wang et al. (2008) |
| Unlabeled hairpin DNA probe in the presence and absence of MutS | Electrochemical impedance spectroscopy | C–C, C–A, C–T, G–A, G–G, G–T, T–T, A–A | 210–1600 | Gong et al. (2009) |
| Electronic transduction and amplification by tagged liposomes | Faradic impedance spectroscopy | G–T | 55 | Patolsky et al. (2001) |
| The Present sensor | Differential pulse voltammetry | G–A,G–T,C–A,T–T | 70 | Present work |

## Acknowledgment

The authors would like to gratefully acknowledge the financial support of this project by the Research Council of University of Isfahan under contract no. 90.698, 90/1/16.

## References

Angnes, L., Richter, E.M., Augelli, M.A., Kume, G.H., 2000. Analytical Chemistry 72 (21), 5503–5506.
Boon, E.M., Ceres, D.M., Drummond, T.G., Hill, M.G., Barton, J.K., 2000. Nature Biotechnology 18 (10), 1096–1100.
Boon, E.M., Salas, J.E., Barton, J.K., 2002. Nature Biotechnology 20 (3), 282–286.
Cai, H., Xu, Y., Zhu, N., He, P., Fang, Y., 2002. Analyst 127 (6), 803–808.
Chang, H., Wang, Y., Li, J., 2011. Current Organic Chemistry 15, 506–517.
Di Giusto, D.A., Wlassoff, W.A., Giesebrecht, S., Gooding, J.J., King, G.C., 2004. Journal of the American Chemical Society 126 (13), 4120–4121.
Fan, C., Plaxco, K.W., Heeger, A.J., 2003. Proceedings of the National Academy of Sciences 100 (16), 9134–9137.
Farjami, E., Clima, L., Gothelf, K., Ferapontova, E.E., 2011. Analytical Chemistry 83, 1594–1602.
Ferreira, A.A.P., Fugivara, C.S., Barrozo, S., Suegama, P.H., Yamanaka, H., Benedetti, A.V., 2009. Journal of Electroanalytical Chemistry 634 (2), 111–122.
Fojta, M., Kostecka, P., Tefulka, M., Havran, L., Palecek, E., 2006. Analytical Chemistry 79 (3), 1022–1029.
Fu, Y., Yuan, R., Xu, L., Chai, Y., Zhong, X., Tang, D., 2005. Biochemical Engineering Journal 23 (1), 37–44.
Gaoa, H.-W., Qinb, P., Lina, C., Shang, Z.-M., Sunb, W., 2010. Journal of the Iranian Chemical Society 7, 119–127.
Ge, D., Levicky, R., 2010. Chemical Communications 46 (38), 7190–7192.
Gong, H., Zhong, T., Gao, L., Li, X., Bi, L., Kraatz, H.-B., 2009. Analytical Chemistry 81 (20), 8639–8643.
Gorodetsky, A.A., Buzzeo, M.C., Barton, J.K., 2008a. Bioconjugate Chemistry 19 (12), 2285–2296.
Gorodetsky, A.A., Ebrahim, A., Barton, J.K., 2008b. Journal of the American Chemical Society 130 (10), 2924–2925.
Gorodetsky, A.A., Green, O., Yavin, E., Barton, J.K., 2007. Bioconjugate Chemistry 18 (5), 1434–1441.
Gorodetsky, A.A., Hammond, W.J., Hill, M.G., Slowinski, K., Barton, J.K., 2008c. Langmuir 24 (24), 14282–14288.
Hook, F., Ray, A., Norden, B., Kasemo, B., 2001. Langmuir 17 (26), 8305–8312.
Hu, K., Lan, D., Li, X., Zhang, S., 2008. Analytical Chemistry 80 (23), 9124–9130.
Ihara, T., Nakayama, M., Murata, M., Nakano, K., Maeda, M., 1997. Chemical Communications 17, 1609–1610.
Jia, F., Yu, C., Ai, Z., Zhang, L., 2007. Chemistry of Materials 19 (15), 3648–3653.
Jia, J., Cao, L., Wang, Z., 2008. Langmuir 24 (11), 5932–5936.
Kelley, S.O., Barton, J.K., Jackson, N.M., Hill, M.G., 1997. Bioconjugate Chemistry 8 (1), 31–37.
Kelley, S.O., Boon, E.M., Barton, J.K., Jackson, N.M., Hill, M.G., 1999a. Nucleic Acids Research 27 (24), 4830–4837.
Kelley, S.O., Jackson, N.M., Hill, M.G., Barton, J.K., 1999b. Angewandte Chemie-International Edition 38 (7), 941–945.
Kiani, A., Fard, E.N., 2009. Electrochimica Acta 54 (28), 7254–7259.
Li, X., Lee, J.S., Kraatz, H.-B., 2006. Analytical Chemistry 78 (17), 6096–6101.
Li, X., Song, H., Nakatani, K., Kraatz, H.-B., 2007. Analytical Chemistry 79 (6), 2552–2555.
Li, X., Zhou, Y., Sutherland, T.C., Baker, B., Lee, J.S., Kraatz, H.-B., 2005. Analytical Chemistry 77 (17), 5766–5769.
Liu, G., Lin, Y., 2007. Journal of the American Chemical Society 129 (34), 10394–10401.
Long, Y.-T., Li, C.-Z., Sutherland, T.C., Kraatz, H.-B., Lee, J.S., 2004. Analytical Chemistry 76 (14), 4059–4065.
Mehrgardi, M.A., Ahangar, L.E., 2011. Biosensors and bioelectronics 26 (11), 4308–4313.
Mehrgardi, M.A., Daneshtalab, R., 2011. Journal of Electroanalytical Chemistry 650 (2), 214–218.
Patolsky, F., Lichtenstein, A., Willner, I., 2001. Journal of the American Chemical Society 123 (22), 5194–5205.
Patolsky, F., Weizmann, Y., Willner, I., 2002. Journal of the American Chemical Society 124 (5), 770–772.
Peterson, A.W., Wolf, L.K., Georgiadis, R.M., 2002. Journal of the American Chemical Society 124 (49), 14601–14607.
Polsky, R., Gill, R., Kaganovsky, L., Willner, I., 2006. Analytical Chemistry 78 (7), 2268–2271.
Rho, S., Jahng, D., Lim, J.H., Choi, J., Chang, J.H., Lee, S.C., Kim, K.J., 2008. Biosensors and bioelectronics 23 (6), 852–856.
Sassolas, A., Leca-Bouvier, B.D., Blum, L.J., 2007. Chemical Reviews 108 (1), 109–139.
Steel, A.B., Herne, T.M., Tarlov, M.J., 1998. Analytical Chemistry 70 (22), 4670–4677.
Vlassiouk, I., Takmakov, P., Smirnov, S., 2005. Langmuir 21 (11), 4776–4778.
Wang, Y., Li, C., Li, X., Li, Y., Kraatz, H.-B., 2008. Analytical Chemistry 80 (6), 2255–2260.
Wong, E.L.S., Gooding, J.J., 2006. Analytical Chemistry 78 (7), 2138–2144.
Wong, E.L.S., Mearns, F.J., Gooding, J.J., 2005. Sensors Actuators B: Chemical 111–112, 515–521.
Xiao, Y., Lou, X., Uzawa, T., Plakos, K.J.I., Plaxco, K.W., Soh, H.T., 2009. Journal of the American Chemical Society 131 (42), 15311–15316.
Xiao, Y., Qu, X., Plaxco, K.W., Heeger, A.J., 2007. Journal of the American Chemical Society 129 (39), 11896–11897.
Yu, C.J., Wan, Y., Yowanto, H., Li, J., Tao, C., James, M.D., Tan, C.L., Blackburn, G.F., Meade, T.J., 2001. Journal of the American Chemical Society 123 (45), 11155–11161.
Zhang, J., Wu, X., Chen, P., Lin, N., Chen, J., Chen, G., Fu, F., 2010. Chemical Communications 46 (37), 6986–6988.
Zhang, R.-Y., Wang, X.-M., Gong, S.-J., He, N.-Y., 2005. Genomics, Proteomics and Bioinformatics 3, 47–51.
Zhong, G., Liu, A., Chen, X., Wang, K., Lian, Z., Liu, Q., Chen, Y., Du, M., Lin, X., 2011. Biosensors and Bioelectronics. 26 (9), 3812–3817.